HOKUGA 北海学園学術情報リポジトリ

タイトル	Precision improvement by polychromatic illumination in displacement measurements of objects based on fractal speckle
著者	Uozumi, Jun
引用	工学研究:北海学園大学大学院工学研究科紀要(25): 17-26
発行日	2025-09-30

研究論文

Precision improvement by polychromatic illumination in displacement measurements of objects based on fractal speckle

Jun Uozumi*

ABSTRACT

In displacement measurements of objects with optically rough surfaces using speckle intensity distributions, fractal speckle patterns offer the potential to significantly extend the measurement range due to the power-law behavior of their intensity correlations. However, a major drawback of this method is that measurements become unstable at large displacements due to increased statistical fluctuations. To overcome this problem, this paper proposes the use of polychromatic illumination and the detection of speckle intensity distributions at multiple wavelengths. By observing a sufficient number of speckle patterns across different wavelengths, statistical fluctuations can be averaged out, thus improving measurement stability in the long-displacement regime. Theoretically, for a sufficiently rough surface, using N wavelengths can reduce statistical fluctuations by a factor of $1/\sqrt{N}$. In practice, however, the actual reduction depends on both the number of wavelengths and the surface roughness of the object being measured. These dependencies and conditions are analyzed through computer simulations.

1. Introduction

In some applications of speckle, spatial correlation properties play a crucial role in their underlying principles.¹⁻³⁾ For such applications, it is beneficial to engineer the speckle field to exhibit long-range spatial correlations. One approach is to generate speckle intensity distributions with fractal characteristics, since fractal intensity patterns inherently exhibit long-range correlations that follow a power-law decay.^{4,5)} An example of such a fractal speckle pattern is shown in fig. 1. This image was obtained through computer simulation, assuming that coherent light with a wavelength of 550 nm is incident on a rough surface whose roughness exceeds the wavelength, resulting in the speckle pattern observed in the image plane. The properties of fractal speckles, both in the diffraction region and in the image plane, have also been extensively investigated by the author and his colleagues.⁴⁻¹⁶⁾ As is seen in fig. 1, fractal speckles do not have a definite grain size but consist of wide range of grains from very tiny ones to large scale clusters, and the size distribution of grains or clusters obeys a power law. This property gives rise to a power-law spatial correlation of the speckle. Therefore, fractal speckles have a possibility to improve measurements based on spatial correlations of speckles.

As an example, fractal correlations have been shown to extend the measurement range in object displacement measurements using speckle patterns.¹⁷⁾ However, displacement measurements with fractal speckles suffer from decreasing precision as the displacement increases. This is because the number of speckle clusters decreases with the cluster size, leading to insufficient statistical averaging at large displacements, as observed in fig. 1.

^{*} Professor Emeritus, Hokkai-Gakuen University

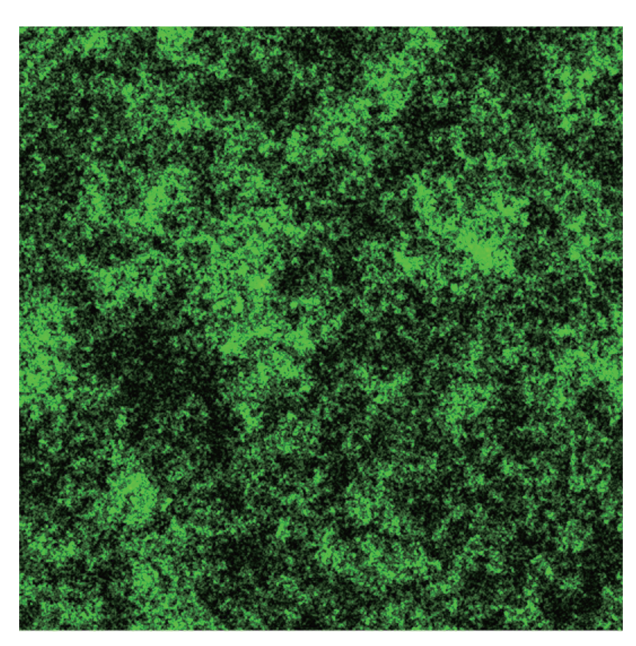


Figure 1 Fractal speckle pattern generated by simulation in the image plane of a rough surface illuminated by coherent light of the wavelength of 550 nm.

To overcome this limitation, we propose the use of spatially coherent polychromatic illumination to enhance the statistical averaging effect. The statistical properties of speckles generated under polychromatic illumination have been extensively studied in the context of fundamental research, ^{18–23)} surface roughness measurements, ^{24–28)} and speckle reduction techniques, ^{29,30)} and so forth. Among the above, the concept of using polychromatic illumination to enhance statistical averaging is basically related to the techniques of speckle reduction.

It is well known that, under monochromatic illumination, when a sufficiently large number of scattering elements contribute to an observation point, the resulting speckle pattern becomes Gaussian, and its statistics are independent of the standard deviation of the phase modulations, provided these modulations exceed 2π . In contrast, under polychromatic illumination, the speckle field exhibits significantly different properties, including continuously varying statistics, even when the phase modulations exceed 2π . This distinct behavior of polychromatic speckles offers a prospective approach to improving the measurement precision in displacement measurements based on fractal speckles. In this paper, we investigate this approach through computer simulations and demonstrate its effectiveness in reducing the precision degradation observed at large displacements.

2. Optical configuration

To utilize fractal speckles for displacement measurement, the speckle pattern must be observed in the image plane of a rough-surface object acting as a diffuser. Accordingly, we assume a double-diffraction optical system, as illustrated in fig. $2.^{17}$ A transparent object with a rough surface is placed in the object plane, and it is illuminated uniformly and normally by spatially coherent polychromatic light. Then, the complex amplitude U_0 of a single wavelength component just after the object can be expressed as

$$U_0(\mathbf{r}_0; \lambda) = \exp[\phi(\mathbf{r}_0; \lambda)], \tag{1}$$

assuming that the incident complex amplitude is unity. In eq. (1), $\mathbf{r}_0 = (x_0, y_0)$ is the coordinate in the object plane, λ is the wavelength of the incident light, and $\phi(\mathbf{r}_0; \lambda)$ is the random phase produced by the rough surface and is given by

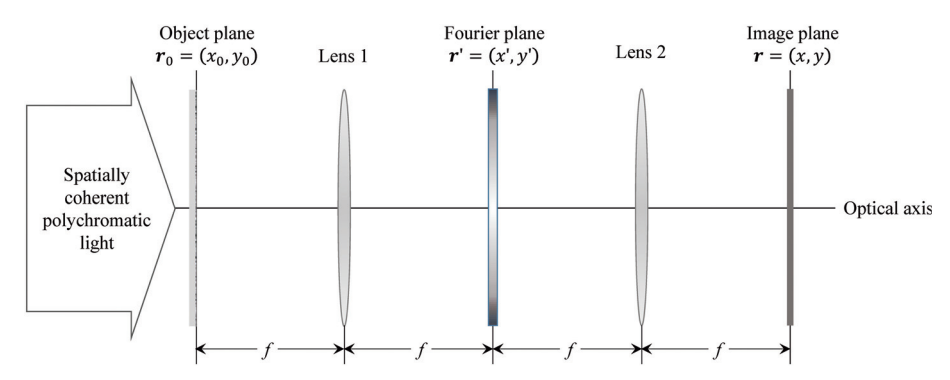


Figure 2 Double diffraction optical system assumed in the simulation. A rough-surface object is placed in the object plane and a filter with power-law amplitude transmittance is located in the Fourier plane.

$$\phi(\mathbf{r}_0; \lambda) = k(n-1) h(\mathbf{r}_0), \tag{2}$$

in which $k = 2\pi/\lambda$ is the wavenumber, n is the refractive index of the rough-surface object, and $h(\mathbf{r}_0)$ is the random height function of the rough surface.³¹⁾ By placing a filter with power-law amplitude transmittance in the Fourier plane of the optical system, the speckle pattern observed in the image plane acquires a fractal intensity distribution. Such a power-law filter can be implemented using a spatial light modulator based on a liquid crystal module or even antique photographic film.

In this optical system, the wave propagation from the object plane to just before the Fourier plane is described by³³⁾

$$U'(\mathbf{r}';\lambda) = \frac{1}{i\lambda f} \iint_{-\infty}^{\infty} U_0(\mathbf{r}_0;\lambda) \exp\left(-i\frac{2\pi}{\lambda f}\mathbf{r}'\cdot\mathbf{r}_0\right) d\mathbf{r}_0, \tag{3}$$

where $U'(\mathbf{r}'; \lambda)$ is the complex amplitude in the Fourier plane, $\mathbf{r}' = (x', y')$ is the coordinate in this plane and f is the focal length of two lenses. The propagation of the wave of the single wavelength from the Fourier pane to the image plane is then expressed by

$$U(\mathbf{r};\lambda) = \frac{1}{i\lambda f} \iint_{-\infty}^{\infty} U'(\mathbf{r}';\lambda) F(\mathbf{r}') \exp\left(-i\frac{2\pi}{\lambda f}\mathbf{r}\cdot\mathbf{r}'\right) d\mathbf{r}',\tag{4}$$

in which $U(\mathbf{r}; \lambda)$ is the complex amplitude in the image plane and $\mathbf{r} = (x, y)$ is the coordinate system in this plane. In eq. (4),

$$F(\mathbf{r}') = r'^{-D/2} \tag{5}$$

is the amplitude transmittance of the power-law filter placed in the Fourier plane and r' = |r'|. D in eq. (5) stands for the exponent of the negative power function as the intensity transmittance, and lies in the range $1 \le D \le 2^{4}$

In this configuration, the speckle intensity distribution $I(\mathbf{r}, \xi; \lambda) = |U(\mathbf{r}, \xi; \lambda)|^2$ is recorded, where ξ is introduced in the arguments of U and I to represent the displacement of the object in the x_0 direction within the object plane. The correlation coefficient between the intensity distributions before and after displacement, namely $I(\mathbf{r}, 0; \lambda)$ and $I(\mathbf{r}, \xi; \lambda)$, respectively, is calculated. The resulting intensity correlation function $C_I(\xi; \lambda)$ characterizes how the speckle pattern changes with displacement ξ and it is observed to decay according to a power law $\xi^{-\alpha}$, where this power-law behavior arises from the fractal nature of the speckle pattern.¹⁷⁾ Accordingly, the displacement distance ξ can be determined from the measured correlation coefficient.

In this measurement system, the exponent α of the negative power function of the intensity correlation is related to the exponent D by

$$\alpha = 2(2 - D),\tag{6}$$

and, therefore, lies in the range $0 \le \alpha \le 2$. The fractal dimension D_s of the speckle pattern is known to be given by $D_s = 2D - 2$.

Since this method relies on variations in speckle patterns produced by different illumination wavelengths to reduce statistical fluctuations, it is necessary to separately detect the speckle pattern corresponding to each wavelength component. This can be achieved either by using multi-wavelength illumination and simultaneous detection for each spectral component, or using continuous polychromatic illumination combined with a spectroscopic imaging system for wavelength-resolved detection.

3. Simulation method

As the height distribution function $h(\mathbf{r}_0)$ of the diffuser, a two-dimensional array of 1024×1024 pixels consisting of zero-mean Gaussian random numbers with a standard deviation σ_h is generated. A sample set of diffusers is prepared by generating one hundred statistically independent random number arrays of this type. The standard deviation of the random phase produced by the diffuser is then given by eq. (2) as $\sigma_{\phi} = 2\pi (n-1)$ σ_h/λ . In the present simulation, the refractive index of the diffuser material is assumed to be n = 1.5, which yields

$$\sigma_{\phi} = \frac{\pi}{\lambda} \, \sigma_{h}. \tag{7}$$

The integrals in eqs. (3) and (4) are evaluated using two-dimensional FFT. In the coordinate systems in the two Fourier transforms, the spatial frequency vectors are defined as

$$f' = (f'_x, f'_y) = \frac{1}{\lambda f}(x', y') = \frac{r'}{\lambda f}$$
 and $f = (f_x, f_y) = \frac{1}{\lambda f}(x, y) = \frac{r}{\lambda f}$, (8)

respectively. However, in the calculation of the correlation function, the spatial frequencies are treated as position vectors $\mathbf{r}' = (\mathbf{x}', \mathbf{y}')$ and $\mathbf{r} = (\mathbf{x}, \mathbf{y})$, respectively, by neglecting the factor $1/(\lambda f)$. This simplification corresponds to ignoring the effect of wavelength-dependent scaling of the diffraction pattern in each optical Fourier transform. Since the observation is performed in the image plane of the object, the final image does not exhibit wavelength-dependent expansion. Thus, ignoring the factor $1/(\lambda f)$ does not affect the result. This is due to the cancellation of the wavelength-dependent scaling effects through the two successive Fourier transforms.

On the other hand, the power-law filter placed in the Fourier plane is affected by the variation of wavelength since its effect appears in the image plane through a single Fourier transform. Specifically, the field of a longer wavelength scattered from the object into the image plane experiences the power-law filter as narrower than that of a shorter wavelength. Expressing this effect by a wavelength-dependent scaling factor $c(\lambda)$, the filter function can be rewritten as

$$F(\mathbf{r}') = [c(\lambda)r']^{-D/2} = c^{-D/2}(\lambda)r'^{-D/2}.$$
(9)

Due to the property of the power functions, scaling the coordinates is equivalent to multiplying the function by a wavelength-dependent factor, which appears in the intensity of the observed image. However, since the intensity correlation function is normalized by its value at the origin, the effect of this factor is eventually eliminated. Therefore, the wavelength-dependent scaling of the filter function does not need to be considered in the simulation. For the same reason of the normalization, the factor in front of the diffraction integrals is also ignored.

The simulation is carried out as follows. Firstly, the intensity distribution $I(\mathbf{r}, 0; \lambda)$ of the image speckle pattern of a single illuminating wavelength λ is calculated using a 512 \times 512 pixel region located at the right-central edge of the diffuser array. This corresponds to placing a rectangular aperture of size 512 \times 512 over that region of the array. Next the aperture is shifted one pixel to the left, corresponding to translating the

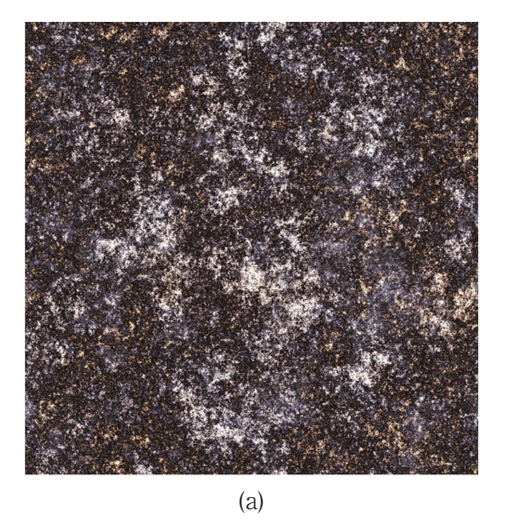
diffuser by $\xi = 1$ in the x_0 direction, and the intensity distribution $I(\mathbf{r}, \xi; \lambda)$ is calculated. From these two intensity distributions, the correlation coefficient is evaluated. By repeating this translation step, increasing ξ up to 512 pixels, the intensity correlation function $C_I(\xi; \lambda)$ is obtained. This correlation function is computed for each diffuser from the sample set of one hundred statistically independent random arrays for six different roughness values $\sigma_h = 2.5$, 5, 10, 20, 40 and 80 μ m. Although a sample size of one hundred is not sufficient for a Monte Carlo simulation of this type, a much larger sample is impractical due to the extremely time-consuming nature of the simulation process which involves repeated translations of the diffuser. Nevertheless, even with the current sample size, several important properties of the proposed method can be demonstrated.

For the illuminating light, we assume the visible spectrum in the range $380 \le \lambda \le 720$ nm. A set of N wavelengths, equally spaced within this range, is used for polychromatic illumination. Simulations are carried out for three values of N=20, 40 and 80. In the calculations, each wavelength obtained by this equal spacing is rounded to the nearest integer value. For monochromatic illumination, a representative wavelength $\lambda_0=550$ nm, corresponding to the center of the visible spectrum is used. An example of the fractal speckle pattern generated using this wavelength is shown in fig. 1.

From the intensity correlation functions $C_I(\xi;\lambda)$ obtained through the above procedure, the standard deviation $\sigma_C(\xi,\lambda_0)$ of the correlation $C_I(\xi;\lambda_0)$ generated by λ_0 is calculated. This quantity characterizes the statistical variation caused by different realization of statistically independent rough surfaces. In addition, a wavelength-averaged correlation function $\langle C_I(\xi;\lambda)\rangle_{\lambda,N}$ is evaluated, where $\langle \cdot \rangle_{\lambda,N}$ stands for averaging over N wavelengths. The standard deviation $\sigma_{\langle C \rangle_{\lambda,N}}(\xi)$ of this averaged correlation calculated from the 100 diffuser realizations is then obtained. The ratio $\sigma_{\langle C \rangle_{\lambda,N}}(\xi)/\sigma_C(\xi;\lambda_0)$ expresses the extent to which polychromatic illumination suppresses statistical fluctuations as a function of ξ . By averaging this ratio over a certain range of ξ , the suppression degree is finally obtained as $R(N,\sigma_h) = \langle \sigma_{\langle C \rangle_{\lambda,N}}(\xi)/\sigma_C(\xi;\lambda_0)\rangle_{\xi}$, where $\langle \cdot \rangle_{\xi}$ denotes the average over the selected range of ξ . This quantity characterizes the effect of polychromatic averaging in reducing statistical noise for each combination of N and σ_h .

4. Results and discussion

Two examples of fractal speckle patterns simulated in the image plane under polychromatic illumination with N=10 wavelengths are shown in figs. 3(a) and (b). In these simulations, the surface roughness of the object is



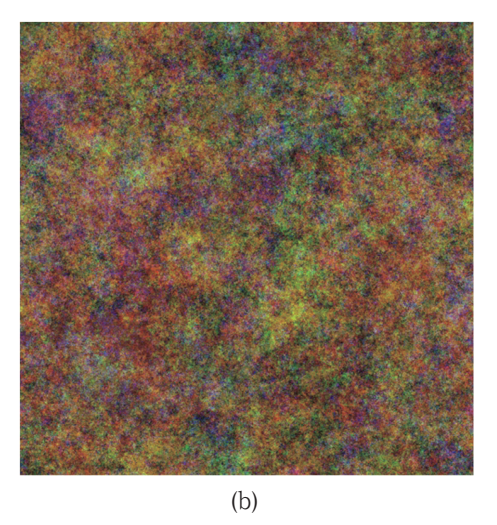


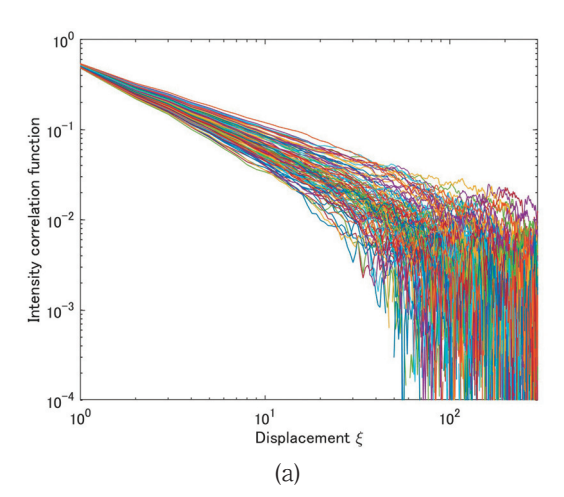
Figure 3 Polychromatic speckles generated by the illumination with N = 10 wavelengths and surface roughness of (a) 0.5 μ m and (b) 5 μ m.

assumed to be (a) $0.5 \,\mu m$ and (b) $5 \,\mu m$. The color speckle patterns presented in figs. 1 and 3 were generated following the simulation procedure described in the author's previous paper⁶⁾. As observed in fig. 3, when the surface roughness is small, speckle pattern produced by different wavelengths are nearly identical, resulting in an almost white polychromatic speckle pattern. However, when the roughness becomes sufficiently large, different wavelengths experience different phase modulations, leading to visibly different patterns, and giving rise to a colorful composite image. These results suggest that, by employing an object with a sufficiently large surface roughness and illuminating it with a sufficiently large number of wavelengths with appropriate separations, one can effectively generate a set of statistically independent speckle patterns to suppress statistical fluctuations in the correlation function.

Figure 4(a) shows the intensity correlation functions $C_I(\xi;\lambda_0)$ at the central wavelength λ_0 = 500 nm computed for 100 rough surfaces with a surface roughness of σ_h = 40 μ m. These results demonstrate that the correlation function fluctuates significantly depending on the specific realization of the rough surface, indicating that displacement measurements using a single object and a single wavelength lack reliability. Figure 4(b) shows the correlation function $\langle\langle C_I(\xi;\lambda)\rangle_{\lambda,N}\rangle_d$, averaged over N=40 wavelengths and 100 rough surfaces realizations, where $\langle \cdot \rangle_d$ denotes the ensemble average over diffuser samples. This figure clearly shows that the intensity correlation function follows a power-law decay over a certain range of the displacement ξ . In the simulation, the exponent of D=1.5 is used. According to eq. (6), the expected exponent of the power-law decay is α =1, which is closely matches the behavior observed in fig. 4(b).

Figure 5(a) shows the standard deviation $\sigma_C(\xi, \lambda_0)$ of the 100 correlations functions $C_I(\xi; \lambda_0)$ shown in fig. 4(a). The black line represents the ensemble-averaged function $\langle C_I(\xi; \lambda_0) \rangle_d$, while the red and green lines indicate the average plus and minus the standard deviation, respectively. Figure 5(b) illustrates the standard deviation $\sigma_{\langle C \rangle_{\lambda,N}}(\xi)$ of the wavelength-averaged correlation function $\langle C_I(\xi; \lambda) \rangle_{\lambda,N}$ computed over N=40 wavelengths. The black line shows the doubly average correlation $\langle \langle C_I(\xi; \lambda) \rangle_{\lambda,N} \rangle_d$, while the red and green lines show this average plus and minus the standard deviation, respectively. These results confirm that averaging over multiple wavelengths significantly suppresses the fluctuations in the intensity correlation function, particularly within the displacement range where the power-law behavior is observed.

The ratio $\sigma_{\langle C \rangle_{\lambda,N}}(\xi)/\sigma_C(\xi;\lambda_0)$ of the two standard deviations shown in figs. 5(a) and (b) is plotted in fig. 6 as a function of ξ , illustrating the degree of the statistical fluctuation suppression due to wavelength averaging. Although random noise increases at larger displacement, where logarithmically displayed correlation function deviates from linearity, due to the limited sample size, the ratio remains relatively



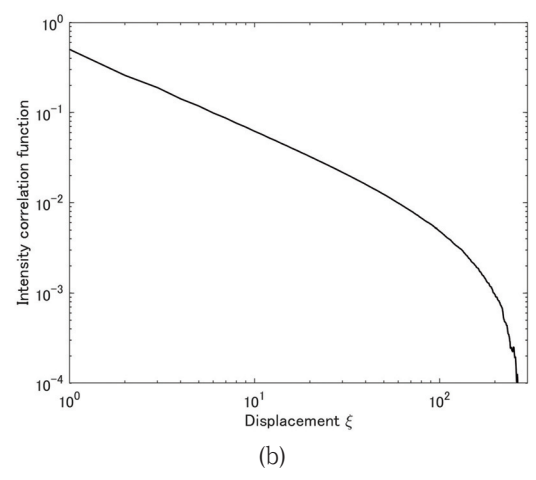
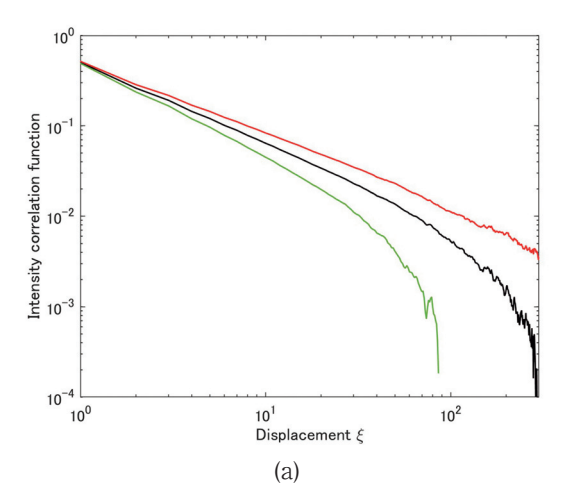


Figure 4 Intensity correlation functions of (a) $C_I(\xi;\lambda_0)$ at the central wavelength λ_0 = 500 nm for 100 rough surfaces having the roughness of σ_h = 40 μ m and (b) $\langle\langle C_I(\xi;\lambda)\rangle_{\lambda,N}\rangle_d$ averaged over N = 40 wavelengths and over 100 rough surfaces.



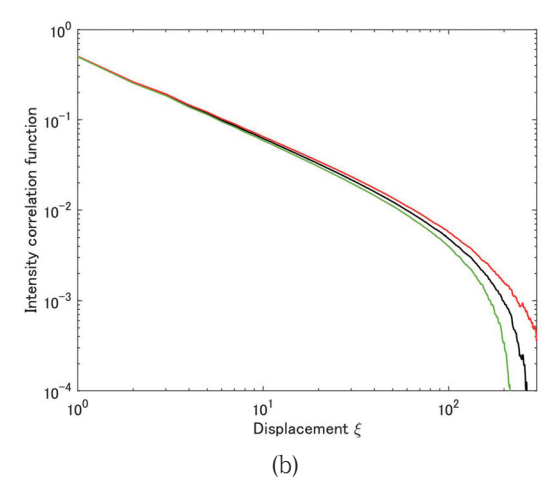


Figure 5 Two standard deviations of (a) $\sigma_C(\xi, \lambda_0)$ of the 100 intensity correlations $C_I(\xi; \lambda_0)$ shown in fig. 4(a), and (b) $\sigma_{\langle C \rangle_{\lambda,N}}(\xi)$ of the intensity correlation $\langle C_I(\xi; \lambda) \rangle_{\lambda,N}$ averaged over N=40 wavelengths. In each figure, the black line represents the average correlation over 100 diffusers, while the red and green lines indicate the average plus and minus the standard deviation, respectively.

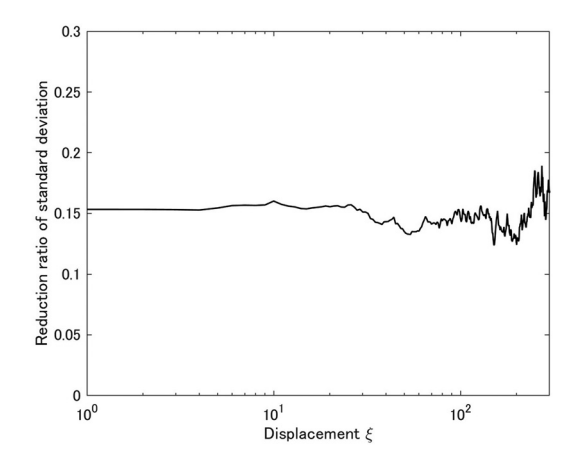


Figure 6 Ratio $\sigma_{\langle C \rangle_{\lambda,N}}(\xi)/\sigma_C(\xi;\lambda_0)$ of the two standard deviations shown in figs. 5(a) and (b).

constant over the displacement range where the correlation function retains its linear behavior.

Therefore, this ratio is averaged over the range $1 \le \xi \le 100$ to obtain the average suppression ratio $R(N, \sigma_h) = \langle \sigma_{\langle C \rangle_{\lambda,N}}(\xi) / \sigma_C(\xi; \lambda_0) \rangle_{\xi}$, which is presented in fig. 7. The results are shown for three values of N = 20, 40 and 80, and six surface roughness values $\sigma_h = 2.5$, 5, 10, 20, 40 and 80 μ m. In the figure, the simulation results are represented by circles. When the surface roughness is sufficiently large such that adjacent wavelengths experience statistically independent phase modulations, the speckles generated by N wavelengths are statistically independent. In this case, the suppression ratio $R(N, \sigma_h)$ is theoretically expected to follow $1/\sqrt{N}$. For the present simulation, the corresponding theoretical values are $1/\sqrt{N} = 0.224$, 0.158 and 0.112 for N = 20, 40 and 80, respectively, and are plotted as solid lines in fig. 7. Although the size of the diffuser sample is insufficient to eliminate fluctuations entirely, the simulation results in fig. 7 are observed to converge approximately to the theoretical values as the roughness σ_h increases.

The wavelength separations in the present simulation are $\Delta \lambda = 17$, 8.8 and 4.25 nm for N = 20, 40 and 80, respectively. The condition under which adjacent wavelengths experience statistically independent phase differences $\Delta \sigma_{\phi}$ can be derived from eq. (7) as

$$\Delta \sigma_{\phi} = \pi \frac{\Delta \lambda}{\lambda^2} \sigma_h > 2\pi, \tag{10}$$

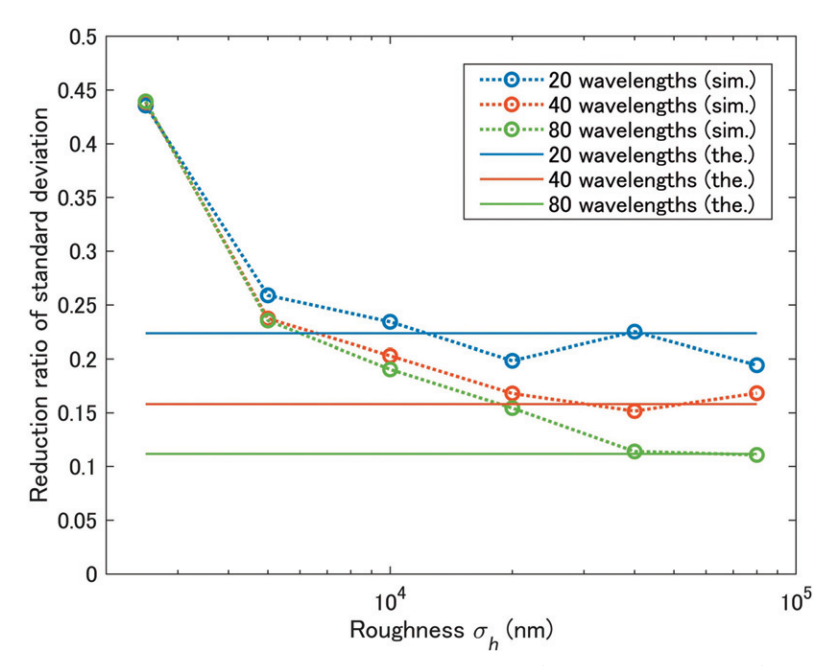


Figure 7 Average suppression ratio $R(N, \sigma_h) = \langle \sigma_{\langle C \rangle_{\lambda, N}}(\xi) / \sigma_C(\xi; \lambda_0) \rangle_{\xi}$ for three sets of wavelengths and six surface roughness values.

from which the required surface roughness is obtained as

$$\sigma_h > \frac{\lambda^2}{2\Delta\lambda}$$
 (11)

Considering the case of the longest wavelength $\lambda = 720$ nm, where the adjacent wavelengths yield the smallest phase difference, eq. (11) gives approximately lower bounds for the surface roughness as $\sigma_h > 15$, 30 and 60 µm for N = 20, 40 and 80, respectively. These values are in good agreement with the roughness thresholds at which the simulation results begin to converge to the theoretical suppression ratios. This result confirms that increasing the number of illuminating wavelengths enhances the suppression of statistical fluctuations in the intensity correlations functions. However, to achieve such high suppression levels, the surface roughness of the diffuser must be sufficiently large to produce statistically independent phase variations between adjacent wavelengths.

5. Conclusion

Fractal speckles produced in the image plane of an optical rough surface have the potential to extend the measurable range of object displacement in methods based on speckles. However, a major drawback of fractal speckle is the fluctuations of its long correlation tail, which varies depending on the specific object being measured.

To overcome this issue, we proposed the use of multi-wavelength illumination of the object. This approach enables the simultaneous generation of multiple statistically independent speckle patterns. If the effective number of independent speckle patterns is N, the statistical fluctuations in the correlation tail can be suppressed by a factor of $1/\sqrt{N}$ theoretically.

Computer simulations were conducted to evaluate the proposed approach for improving the precision of the displacement measurement. The optical system was modeled as a double diffraction system, with a diffuser placed in the object plane and a filter of a power-law amplitude transmittance located in the Fourier plane. The power-law exponent of the amplitude transmittance was set to D/2 with D=1.5. Simulations were

carried out for a sample set of one hundred statistically independent diffusers. Displacement measurement was performed by calculating the intensity correlations between speckle patterns before and after the displacement.

For illumination wavelengths λ , three sets of N=20, 40 and 80 wavelengths were selected, equally spaced over the range $380 \le \lambda \le 720$ nm. Six different surface roughness values $\sigma_h=2.5$, 5, 10, 20, 40 and 80 μ m for the diffusers were examined. Intensity correlations computed from a single speckle pattern generated by monochromatic illumination at $\lambda=550$ nm, the central wavelength of the assumed range, exhibited largely fluctuations across different diffusers.

It was shown that averaging the correlation functions over N wavelengths significantly suppressed these fluctuations. Furthermore, the resulting averaged correlation function decayed following a power-law with an exponent close to the theoretical prediction. The suppression effect was found to be nearly constant over the displacement range ξ in which the correlation function obeys the power law. By averaging the suppression ratio over this displacement range, a single representative value $R(N, \sigma_h)$ was obtained for each combination of N and σ_h . Finally, it was confirmed that $R(N, \sigma_h)$ decreases with increasing surface roughness and asymptotically approaches the theoretical value of $1/\sqrt{N}$ for sufficiently large σ_h .

References

- 1) G. P. Weigelt: Real time measurement of the motion of a rough object by correlation of speckle patterns, Opt. Commun., 19, 2, pp. 223–228, 1976.
- 2) R. K. Erf, ed.: Speckle Metrology, Academic, New York, 1978.
- 3) R. S. Sirohi, ed.: Selected Papers on Speckle Metrology, SPIE Milestone Series Vol. MS 35, SPIE, Washington, 1991.
- 4) K. Uno et al.: Correlation properties of speckles produced by diffractal-illuminated diffusers, Opt. Commun., 124, 1-2, pp. 16-22, 1996.
- 5) J. Uozumi et al.: Fractal speckles, Opt. Commun., 156, 4-6, pp. 350-358, 1998.
- 6) J. Uozumi: Fractal speckles produced by polychromatic illumination —Computer simulation— (in Japanese), Engineering Research (Bull. Grad. Sch. Eng., Hokkai-Gakuen Univ.), No. 8, pp. 63-74, 2008.
- 7) J. Uozumi: Generation and properties of laser speckle with long correlation tails, Proc. SPIE 4705 (Saratov Fall Meeting 2001: Coherent Optics of Ordered and Random Media II) pp. 95–106, 2002.
- 8) J. Uozumi: Fractality of the optical fields scattered by power-law-illuminated diffusers, Proc. SPIE 4602 (Fifth International Conference on Correlation Optics), pp. 257–267, 2002.
- 9) H. Funamizu and J. Uozumi: Generation of fractal speckles by means of a spatial light modulator, Opt. Express, 15, 12, pp. 7415–7422, 2007.
- 10) J. Uozumi: Phase singularity distribution of fractal speckles, Proc. 2nd Internat. Conf. Optics and Laser Applications (ICOLA'07), Yogyakarta, Indonesia, pp. 16–20, 2007.
- 11) H. Funamizu and J. Uozumi: Multifractal analysis of speckle intensities produced by power-law illumination of diffusers, J. Modern Opt., 54, 10–12, pp. 1511–1528, 2007.
- 12) H. Funamizu and J. Uozumi: Scaling reduction of the contrast of fractal speckles detected with a finite aperture, Opt. Commun., 281, 4, pp. 543–549, 2008.
- 13) M. Ibrahim and J. Uozumi: Three-dimensional correlation properties of speckles produced by diffractal-illuminated diffusers, Asian J. Phys., 27, 9–12, pp. 457–466, 2018.
- 14) K. Tsujino and J. Uozumi: Correlation properties of fractal speckles in the Fresnel diffraction region, Asian J. Phys., **27**, 9–12, pp. 515–528, 2018.
- 15) H. Funamizu and J. Uozumi: Statistics of derivatives of intensity and phase of fractal speckles, Asian J. Phys., **27**, 9–12, pp. 563–571, 2018.
- 16) J. Uozumi: Properties of computer-simulated fractal speckles, Engineering Research (Bull. Grad. Sch. Eng., Hokkai-Gakuen Univ.), No. 21, pp. 3–17, 2021.

- 17) E. Miyasaka and J. Uozumi: Generation of fractal speckles in image plane and their application to the measurement of displacement, Engineering Research (Bull. Grad. Sch. Eng., Hokkai-Gakuen Univ.), No. 12, pp. 13–23, 2012.
- 18) G. Parry: Some effects of temporal coherence on the first order statistics of speckle, Opt. Acta, 21, 10, pp. 763-772, 1974.
- 19) K. Nakagawa and T. Asakura: Average contrast of white-light image speckle patterns, Opt. Acta, 26, 8, pp. 951-960, 1979.
- 20) G. Parry: Speckle patterns in partially coherent light, in Laser Speckle and Related Phenomena, ed. J. C. Dainty (Second Enlarged Edition), chap. 3, pp. 77–122, Springer, Berlin, 1984.
- 21) Y. Tomita et al.: Fibrous radial structure of speckle patterns in polychromatic light, Appl. Opt., 19, 18, pp. 3211-3218, 1980.
- 22) Y. Tomita et al.: The contrast of polychromatic speckle patterns at the far-field diffraction region, Canad. J. Phys., 58, 10, pp. 1439–1445, 1980.
- 23) J. Uozumi and Y. Sakai: Statistical analysis of colors in computer-simulated polychromatic speckles (in Japanese), Engineering Research (Bull. Grad. Sch. Eng., Hokkai-Gakuen Univ.), No. 20, pp. 3–21, 2020.
- 24) R. A. Sprague: Surface roughness measurement using white light speckle, Appl. Opt., 11, 12, pp. 2811-2816, 1972.
- 25) G. Tribillon: Correlation entre deux speckle obtenus avec deux longueurs d'onde application a la mesure de la rugosite moyenne, Opt. Commun., 11, 2, pp. 172-174, 1974.
- 26) H. M. Pedersen: On the contrast of polychromatic speckle patterns and its dependence on surface roughness, Opt. Acta, 22, 1, pp. 15–24, 1975.
- 27) K. Nakagawa and T. Asakura: Contrast dependence of white light image speckles on surface roughness, Opt. Commun., 27, 2, pp. 207–213, 1978
- 28) M. Giglio et al.: Surface roughness measurements by means of speckle wavelength decorrelation, Opt. Commun., 28, 2, pp. 166–170, 1979.
- 29) T. S. McKechnie: Speckle reduction, in Laser Speckle and Related Phenomena, ed. J. C. Dainty (Second Enlarged Edition), chap. 4, pp. 123–170, Springer, Berlin, 1984.
- 30) K. Kuroda: Color speckle in laser displays, Proc. SPIE 9659, p. 161, 2015
- 31) J. W. Goodman: Statistical properties of laser speckle pattern, in Laser Speckle and Related Phenomena, ed. J. C. Dainty (Second Enlarged Edition), chap. 2, pp. 9–75, Springer, Berlin, 1984.
- 32) J. Uozumi and T. Asakura: First-order intensity and phase statistics of Gaussian speckle produced in the diffraction region, Appl. Opt., **20**, 8, pp. 1454–1466, 1981.
- 33) J. W. Goodman: Introduction to Fourier Optics (Fourth Edition), Freeman, New York, 2017.